Journal of Photochemistry and Photobiology A: Chemistry 217 (2011) 242–248

Contents lists available at ScienceDirect

Journal of Photochemistry and Photobiology A: Chemistry

journal homepage: www.elsevier.com/locate/jphotochem

Reorganization energy of supramolecular donor–acceptor dyad of octaethylporphyrin isomers and axial-coordinated acceptor: Experimental and computational study

Mamoru Fujitsuka [a], Hisashi Shimakoshi [b], Yoshio Hisaeda [b], Tetsuro Majima [a,*]

[a] The Institute of Scientific and Industrial Research (SANKEN), Osaka University, Mihogaoka 8-1, Ibaraki, Osaka 567-0047, Japan
[b] Department of Chemistry and Biochemistry, Graduate School of Engineering, Kyushu University, Fukuoka 819-0395, Japan

ARTICLE INFO

Article history:
Received 2 September 2010
Received in revised form 6 October 2010
Accepted 15 October 2010
Available online 23 October 2010

Keywords:
Electron transfer
Reorganization energy
Porphyrin
Porphycene
Hemiporphycene
Marcus theory

ABSTRACT

The internal reorganization energy (λ_V) of photoinduced electron transfer (ET) in the supramolecular donor–acceptor dyads of 2,3,7,8,12,13,17,18-octaethylporphinatozinc(II) (ZnOEP) and electron acceptor ligands was compared with those of structural isomers, 2,3,7,8,11,12,17,18-octaethylhemiporphycenatozinc(II) (ZnHPc) and 2,3,6,7,12,13,16,17-octaethylporphycenatozinc(II) (ZnPcn). First, ET process of the supramolecular donor–acceptor dyads of ZnOEP was investigated by means of the transient absorption spectroscopy mainly. The formation of supramolecular dyads was confirmed by absorption spectral change, from which the association constant was estimated. The ET process was confirmed by the observation of radical cation of ZnOEP during the laser flash photolysis. The ET rates of these dyads are in the order of ZnOEP > ZnHPc > ZnPcn, when the driving forces for ET are similar to each other. From the free energy dependence of ET rates, the λ_V values of OEP and its isomers were estimated. The estimated λ_V value was in the order of ZnOEP < ZnHPc < ZnPcn. This tendency was reproduced by calculation at B3LYP/6-31G(d) and BHandHLYP/6-31G(d) levels. The origin of this tendency was discussed on the basis of the structural change during the ET process.

1. Introduction

Porphyrin derivatives have been used as a key pigment to develop various photofunctional and photoactive materials including artificial photosynthesis systems, photocatalyst, photo dynamic therapy, and so on [1]. Preparation of porphyrin derivatives with desirable functions has been carried out by various synthetic methods. Self-assembling by a coordination bond formation to a central metal ion of porphyrin ring is also a useful method to prepare various functional materials using porphyrin derivatives. To date, a number of chromophore arrays including porphyrins prepared by the supramolecular method have been reported [2–4]. Donor–acceptor dyads for efficient photo-energy conversion have been also prepared by means of coordination bonding formation of porphyrin derivatives [5–22].

Recently, we reported the electron transfer (ET) processes of supramolecular donor–acceptor dyads of 2,3,6,7,12,13,16,17-octaethylporphycenatozinc(II) (ZnPcn) and 2,3,7,8,11,12,17,18-octaethylhemiporphycenatozinc(II) (ZnHPc) [23,24], which are structural isomers of 2,3,7,8,12,13,17,18-octaethylporphinatozinc(II) (ZnOEP) (Fig. 1). These isomers have a large absorption in the red and near-IR regions because of their lower symmetry compared to porphyrins [25]. Their redox properties can be controlled by the selection of metal ion in the inner cavity like porphyrins [26]. These points are attractive from the viewpoint of various applications indicated above. As the electron acceptor of these supramolecular dyads, we prepared pyromellitic imide and phthalimide derivatives bearing a pyridine ring (Fig. 1), of which N atom can coordinate to the central Zn ion of these isomers [23,24,27]. From the observed charge separation (CS) and recombination (CR) rates, we have indicated the difference in the electronic coupling and reorganization energy among these isomers, although of which origin was not clarified. Furthermore, the lack of the ET rates in the supramolecular donor–acceptor dyads using ZnOEP and acceptors, which have been employed for dyads using ZnPcn and ZnHPc, limited detailed analysis of these ET processes. Although Otsuki et al. reported that free energy dependence of ET rate between 5,10,15,20-tetraphenylporphyrinatozinc(II) (ZnTPP) and coordinated phthalimides [22], the parameters for ET such as reorganization energy have not been determined. Furthermore, there are difference in participating molecular orbital (MO) to ET between ZnTPP and ZnOEP (a_{1u} and a_{2u}, respectively), and

* Corresponding author. Tel.: +81 6 6879 8495; fax: +81 6 6879 8499.
E-mail address: majima@sanken.osaka-u.ac.jp (T. Majima).

1010-6030/$ – see front matter © 2010 Elsevier B.V. All rights reserved.
doi:10.1016/j.jphotochem.2010.10.016

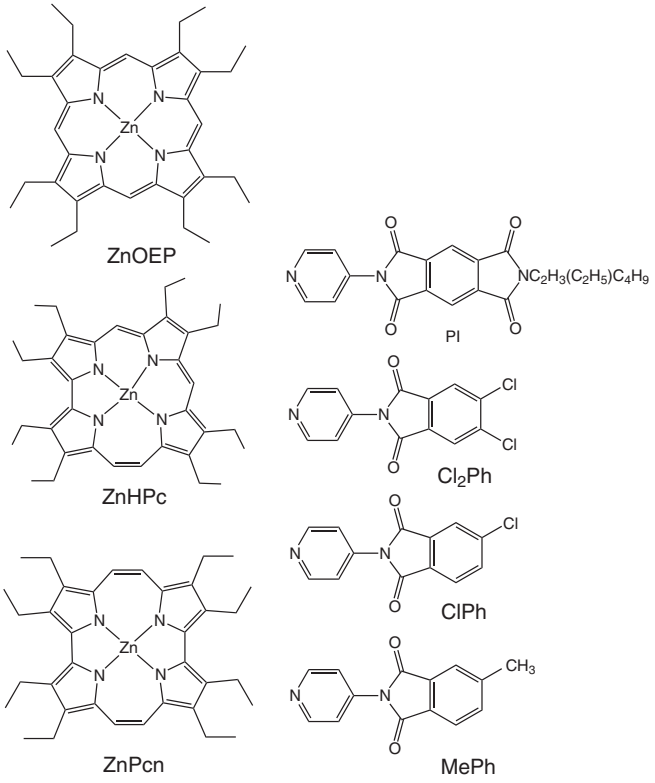

Fig. 1. Molecular structures of ZnOEP, ZnHPc, ZnPcn, PI, and phthalimides.

the molecular structures of electron acceptors are also different from ours. Thus, systematic study on ZnOEP using the same set of electron acceptor ligand as the studies on ZnPcn and ZnHPc is essential to elucidate of isomeric structure-dependence of ET behavior.

In the present paper, ET processes of donor–acceptor dyads of ZnOEP are investigated in order to clear the characteristics of these porphyrin isomers in ET processes depending on its structure. Difference in the ET processes of these isomers is discussed on the basis of the Marcus theory. The MO and structural information obtained by MO calculation of these isomers gave better understanding of the different ET behavior of these isomers.

2. Experimental

2.1. Materials

ZnOEP was purchased from Aldrich and used as received. Axial ligands were prepared as described in the previous papers [23,27]. All spectroscopic studies have been carried out using spectroscopic grade toluene as solvent.

2.2. Apparatus

The subpicosecond transient absorption spectra were measured by the pump and probe method using a regeneratively amplified titanium sapphire laser as reported previously [28]. In the present study, the sample was excited using a 565-nm laser pulse, which was generated by an optical parametric amplifier.

The fluorescence decay profiles were measured by the single photon counting method using a streakscope [29]. The ultrashort laser pulse was generated by a Ti:sapphire laser. For excitation of the sample, the output of the Ti:sapphire laser was converted to the second harmonic oscillation (420 nm) using a harmonic generator.

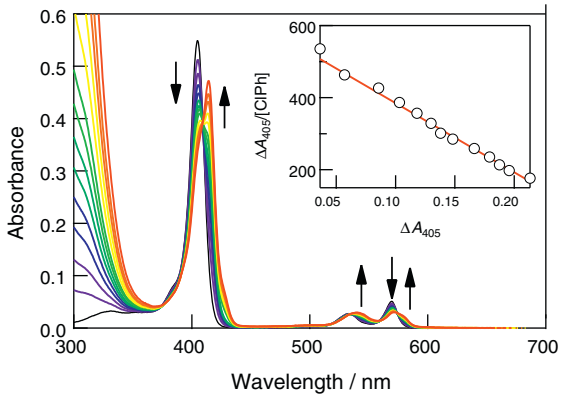

Fig. 2. Steady state absorption spectra of ZnOEP (2.8 μM) in toluene (black line, optical path: 5.0 mm). Spectral changes during the complexation with ClPh was also indicated (concentration of ClPh: 68.0, 135, 201, 267, 331, 395, 458, 520, 642, 761, 877, 990, and 1100 μM). Inset: the Scatchard plot of absorbance at 405 nm.

The steady state absorption and fluorescence spectra were measured using a Shimadzu UV-3100PC and Hitachi 850, respectively.

Optimized structures were estimated at the B3LYP/6-31G(d) and BHandHLYP/6-31G(d) levels using the Gaussian 03 package [30]. For simplicity of the calculation, alkyl groups of the compounds were reduced to methyl groups. The geometries were optimized with tight option using tight SCF convergence and an ultrafine integral grid.

3. Results and discussion

3.1. Electron transfer in supramolecular donor–acceptor dyad of ZnOEP

The supramolecular donor–acceptor dyad of ZnOEP was obtained by the ligation of the electron acceptor bearing a pyridine (Py) ring (Fig. 1), of which N atom can coordinate to the central Zn ion of ZnOEP. The formation of the dyad was confirmed by absorption spectral change. In Fig. 2, the absorption spectral change during the formation of the donor–acceptor dyad of ZnOEP and ClPh in toluene by stepwise addition of ClPh to ZnOEP was indicated as a representative. ZnOEP in toluene shows absorption peaks at 405, 533, and 570 nm. The 405 nm band is the B band and 533 and 570 nm bands are the Q band. Upon addition of ClPh, absorption bands attributable to the dyad by coordination bonding appeared at longer wavelength side of the corresponding bands, i.e., the B- and Q-bands of the dyad appeared at 414 and 541 and 576 nm, respectively. During the spectral change, isosbestic points were observed at 372, 409, 518, 535, 558, and 574 nm. The absorption peak positions of the dyad are the same as those of the Py-coordinated ZnOEP (Table 1), supporting the formation of supramolecular dyad by axial ligation of the Py ring of the acceptor. The constant for the formation of axial-ligated ZnOEP was estimated to be 1920 M^{-1} for ClPh-ZnOEP by applying the Scatchard plot to the absorption change

Table 1
The peak position of the absorption bands (λ_{max}), association constant (K_a), and fluorescence lifetime (τ_F) of ZnOEP complexes in toluene.

Donor	Acceptor	λ_{max}/nm	K_a/M^{-1}	τ_F/ns
ZnOEP	–	405, 533, 570	–	2.0 (100%)
ZnOEP	PI[a]	414, 542, 576	2500	<0.03 (95%), 1.9 (5%)
ZnOEP	Cl_2Ph	414, 541, 576	1860	0.18 (95%), 1.9 (5%)
ZnOEP	ClPh	415, 542, 576	1920	0.51 (91%), 2.0 (9%)
ZnOEP	MePh	415, 542, 576	2050	2.2 (100%)
ZnOEP	Py[a]	415, 542, 577	2200	2.1 (100%)

[a] From Ref. [27].

Table 2
The driving forces and electron transfer rates of ZnOEP, ZnPcn, and ZnHPc in toluene.

Donor	Acceptor	$-\Delta G_{CS}$/eV[a]	$-\Delta G_{CR}$/eV[a]	k_{CS}/s^{-1}[b]	k_{CR}/s^{-1}[b]
ZnOEP	PI	0.83	1.30	1.1×10^{11}	2.7×10^{9}
ZnOEP	Cl_2Ph	0.24	1.89	5.0×10^{9}	2.9×10^{8}
ZnOEP	ClPh	0.12	2.01	1.5×10^{9}	7.0×10^{8}
ZnOEP	MePh	−0.02	2.15	–[c]	–[c]
ZnHPc	PI	0.86	1.15	2.8×10^{10}	3.6×10^{9}
ZnHPc	Cl_2Ph	0.27	1.74	7.6×10^{8}	–[c]
ZnHPc	ClPh	0.15	1.86	0.7×10^{8}	–[c]
ZnHPc	MePh	0.01	2.00	–[c]	–[c]
ZnPcn	PI	0.69	1.19	6.8×10^{9}	2.4×10^{9}
ZnPcn	Cl_2Ph	0.10	1.78	2×10^{7}	–[c]
ZnPcn	ClPh	−0.02	1.90	–[c]	–[c]
ZnPcn	MePh	−0.16	2.04	–[c]	–[c]

[a] For the calculation of ΔG_{CS} and ΔG_{CR} values of ZnOEP supramolecular dyads, following parameters were employed. E(ZnOEP-Py/ZnOEP$^{\bullet+}$-Py) = 0.61 V vs. SCE. $E(A^{\bullet-}/A)$ = −0.83, −1.44, −1.56, and −1.70 V vs. SCE for A = PI, Cl_2Ph, ClPh, and MePh, respectively. $\Delta E_{0\text{-}0}$ = 2.13 eV. The ionic radii of cation, phthalimides, and PI were 5.0, 3.5, and 3.0 Å, respectively. The center to center distances for ZnOEP-PI and ZnOEP-Ph were 9.8 and 8.6 Å, respectively. ΔG_S values were reduced by 0.35 eV according to Ref. [33].
[b] ET rates of PI-ZnOEP are from Ref. [27]. ET rates of dyads of ZnHPc are from Ref. [24]. ET rates of dyads of ZnPcn are from Ref. [23].
[c] Not observed.

at 405 nm (inset of Fig. 2) [31]. The estimated value is similar to that of ZnOEP-Py (Table 1). For other electron acceptors bearing a Py ring, the formation of supramolecular donor–acceptor dyad was confirmed by similar manner. Table 1 summarizes the observed absorption maxima and estimated association constants. These values are similar to each other.

The fluorescence intensity of pentacoordinated ZnOEP depends largely on the acceptor-ability of the ligands. For ZnOEP coordinated by the electron acceptors with higher electron acceptor ability, essentially no fluorescence was observed upon excitation of the absorption band of ZnOEP, while strong fluorescence was observed with the dyad coordinated by Py or MePh with low electron acceptor-ability. This tendency was confirmed by fluorescence lifetime measurement as summarized in Table 1. For the supramolecular dyads, fluorescence decayed according to two components decay, of which shorter component can be attributed to the coordinated ZnOEP while the longer component can be attributed to non-coordinated ZnOEP from the same lifetime as ZnOEP. The fluorescence lifetime became shorter with increase in the electron acceptor ability of the ligand. This observation suggests the contribution of ET from the singlet excited state of ZnOEP.

For better understanding of fluorescence lifetime dependent on the electron acceptor ability of the ligands, the driving forces for the electron transfer (ΔG_{CS} and ΔG_{CR}) were estimated using Weller's equation (Eqs. (1)–(3)) [32] using the electrochemical and spectroscopic data summarized in the footnote of Table 2.

$$-\Delta G_{CS} = \Delta E_{0\text{-}0} - (-\Delta G_{CR}) \quad (1)$$

$$-\Delta G_{CR} = E_{OX} - E_{red} + \Delta G_S \quad (2)$$

$$\Delta G_S = \frac{e^2}{4\pi\varepsilon_0}\left[\left(\frac{1}{2r_D} + \frac{1}{2r_A} - \frac{1}{r}\right)\left(\frac{1}{\varepsilon_s}\right) - \left(\frac{1}{2r_D} + \frac{1}{2r_A}\right)\left(\frac{1}{\varepsilon_r}\right)\right] \quad (3)$$

where $\Delta E_{0\text{-}0}$ is excitation energy, r_D and r_A are ionic radii of donor and acceptor, respectively, r is center-to-center distance, and ε_s are ε_r are dielectric constants of solvent for the rate measurements and redox measurements, respectively. The ΔG_S value was reduced by 0.35 eV according to Ref. [33]. The estimated ΔG values were summarized in Table 2. Although ΔG_{CS} value of ZnOEP–MePh dyad is positive, sufficiently negative ΔG_{CS} values were obtained for other supramolecular dyads. Furthermore, the fluorescence lifetime became shorter with the increase in $-\Delta G_{CS}$ value, supporting the CS from the singlet excited ZnOEP.

The CS and CR processes in the supramolecular donor–acceptor dyads were confirmed by the sub-picosecond transient absorption spectroscopy. Fig. 3 is the transient absorption spectra of ZnOEP–Cl_2Ph in toluene during the laser flash photolysis using 565 nm femtosecond laser pulse for excitation of ZnOEP moiety of the supramolecular dyad. In the present transient absorption study, excess amount (100 equiv.) of the electron acceptor was added to ZnOEP solution to ensure that photoinduced processes of the pentacoordinated form can be elucidated. Under this condition, >99% of ZnOEP is in the pentacoordinated form. The absorption spectrum at 40 ps after the laser excitation can be attributed to the singlet excited state of ZnOEP. With the decay of the singlet excited state of ZnOEP, the absorption band attributable to the radical cation of ZnOEP appeared around 630 nm [34], which showed a rising kinetic trace with the rate equivalent to the fluorescence decay lifetime, indicating that the charge separated state was generated from the singlet excited state of ZnOEP. The rate constant for the CS was estimated from the difference between the reciprocal of fluorescence lifetimes of Py–ZnOEP and Cl_2Ph–ZnOEP to be 5.0×10^9 s^{-1}. The decay of the charge separated state can be attributed to the CR process, of which rate was estimated form the kinetic trace of the transient absorption at 630 nm to be 2.9×10^8 s^{-1}, which corresponds to 3.4 ns of CS lifetime. Similar transient absorption spectral change was observed with ZnOEP–ClPh, while ZnOEP–MePh did not show spectral change due to CS process, which can be rationalized from the endothermic driving force (Table 2). The rate constants for the CS and CR observed with the supramolecular donor–acceptor dyads of ZnOEP were summarized in Table 2. The CS rate constants of ZnOEP–Cl_2Ph and ZnOEP–ClPh were smaller than that of ZnOEP–PI [27]. This observation is explained from the fact that the $-\Delta G_{CS}$ value of ZnOEP–PI is the largest among those of ZnOEP dyads investigated in this study.

3.2. Driving-force dependence of the electron transfer rates

In the previous papers, we have reported the CS and CR rates of the supramolecular dyads of ZnPcn and ZnHPc with the same set of the axial ligands which act as electron acceptors [23,24]. The rate constants for CS and CR (k_{CS} and k_{CR}, respectively)

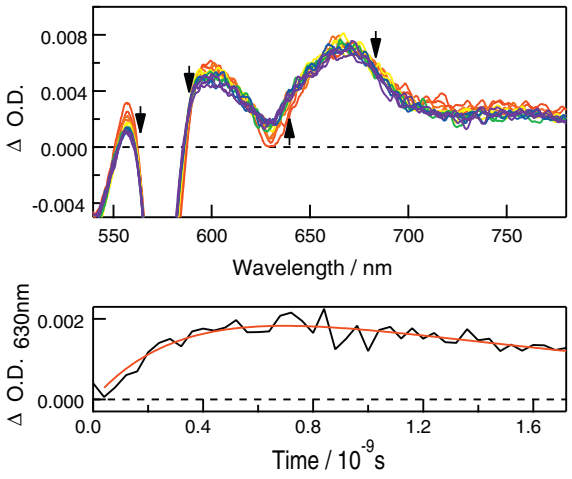

Fig. 3. Transient absorption spectra of Cl_2Ph–ZnOEP in toluene during the laser flash photolysis using 565-nm femtosecond pulse for excitation. Spectra were obtained from 40 to 520 ps (40 ps step) after the laser excitation. Lower panel is kinetic trace of ΔO.D. at 630 nm during the laser flash photolysis. Red curve is a fitted curve. (For interpretation of the references to color in this figure legend, the reader is referred to the web version of the article.)

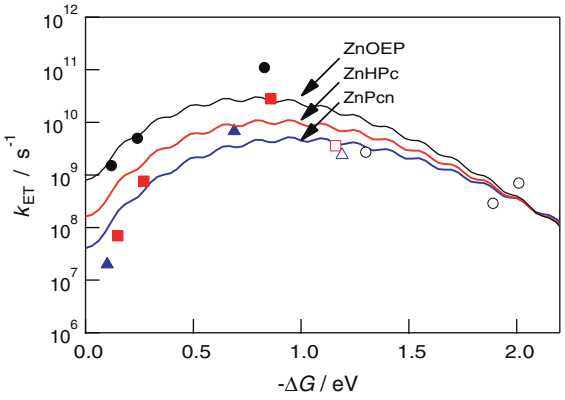

Fig. 4. Free energy change ($-\Delta G$) dependence of ET rate (k_{ET}, i.e., k_{CS} (filled mark) and k_{CR} (opened mark)) of ZnOEP (black circle), ZnPcn (blue triangle), and ZnHPc (red square) complexes. Parameters for each curve were given in Table 3. (For interpretation of the references to color in this figure legend, the reader is referred to the web version of the article.)

Table 3
Parameters of Marcus equation (Eqs. (4)–(6) in text).[a]

Donor	V/meV	λ_V/eV	λ_S/eV	$\hbar\langle\omega\rangle$/eV
ZnOEP	1.6	0.8	0.050	0.15
ZnHPc	1.0	0.9	0.050	0.15
ZnPcn	0.7	1.0	0.050	0.15

[a] Parameters for ZnHPc and ZnPcn were determined in Refs. [23,24].

were summarized as well as the driving forces in Table 2. Previously, we have pointed out that k_{CS} values were in the order of ZnOEP > ZnHPc > ZnPcn for the supramolecular dyads with PI although the $-\Delta G_{CS}$ were similar to each other [23,24]. This tendency was also confirmed with the supramolecular dyads using Cl_2Ph or ClPh as the ligand.

For detailed comparison, the estimated electron transfer rates (k_{ET}, i.e., k_{CS} and k_{CR}) of ZnOEP, ZnHPc, and ZnOEP supramolecular dyads were plotted against the driving forces (ΔG) in Fig. 4. In the previous papers [23,24], we have analyzed the driving force dependence of ET rates based on the Marcus theory, Eqs. (4)–(6) [35,36],

$$k_{ET} = \sqrt{\frac{\pi}{\hbar^2\lambda_S k_B T}}|V|^2\sum_m (e^{-S}(S^m/m!)) \times \exp\left(-\frac{(\lambda_S + \Delta G + m\hbar\langle\omega\rangle)^2}{4\lambda_S k_B T}\right) \quad (4)$$

$$\lambda_S = e^2\left(\frac{1}{2r_D} + \frac{1}{2r_A} - \frac{1}{r}\right)\left(\frac{1}{n^2} - \frac{1}{\varepsilon_S}\right) \quad (5)$$

$$S = \frac{\lambda_V}{\hbar\langle\omega\rangle}. \quad (6)$$

In Eq. (4), λ_S is the solvent reorganization energy given by Eq. (5), V is the electronic coupling, S is the electron-vibration coupling constant given by Eq. (6), and $\langle\omega\rangle$ is the averaged angular frequency. In Eq. (5), n is the refractive index. In Eq. (6), λ_V is the internal reorganization energy. The λ_S value was estimated to be 0.05 eV [23,24]. For ZnPcn and ZnHPc, red and blue curves, respectively, were estimated to reproduce the estimated ET rates using the parameters listed in Table 3. For the supramolecular dyads of ZnOEP, 1.6 meV of the V and 0.8 eV of the λ_V values were employed to obtain the black curve in Fig. 4. Thus, the V value of the ET of porphyrin isomers is in the order of ZnOEP > ZnHPc > ZnPcn, while the λ_V value is ZnPcn > ZnHPc > ZnOEP.

Table 4
Calculated internal reorganization energy (unit: meV).

	B3LYP/6-31G(d)			BHandHLYP/6-31G(d)		
	λ_n[a]	λ_{ion}[b]	λ_V[c]	λ_n[a]	λ_{ion}[b]	λ_V[c]
ZnOEP	32	30	62	43	62	105
ZnHPc	87	10	97	53	60	113
ZnPcn	133	126	259	162	218	380
Py–ZnOEP	94	13	104	67	72	139
Py–ZnHPc	142	32	174	93	68	161
Py–ZnPcn	195	184	379	255	195	450
PI	255	253	508	313	303	616
Cl_2Ph	303	280	583	345	322	667
ClPh	293	294	587	355	335	690
MePh	294	321	615	358	348	705

[a] Energy difference between radical ion and neutral geometries with charge zero.
[b] Energy difference between neutral and radical ion geometries with charge +1 or −1.
[c] Sum of λ_n and λ_{ion}.

For the detailed understanding of the observed differences in V and λ_V values of ET rates of the supramolecular dyads of ZnOEP, ZnHPc, and ZnPcn, MO and molecular structures were investigated by means of MO calculations [24]. It has been pointed out that ET rates from the excited porphyrinoids relate to HOMO electronic densities [37–39]. In the previous paper [24], we showed that the distribution of the HOMO electron density give a plausible explanation for the variation in the V value for ET dependent on porphyrinoids for supramolecular donor–acceptor dyads. That is, the shorter (longer) distance between the acceptor and the carbon with the largest HOMO electron density accelerates (decelerates) ET in supramolecule of ZnOEP (ZnPcn).

According to the Marcus cross relation [35,36,40], reorganization energy of ET process, $D + A \rightleftharpoons D^{\bullet+} + A^{\bullet-}$, is the average of the reorganization energies of following two self-exchange ET processes: $D + D^{\bullet+} \rightleftharpoons D^{\bullet+} + D$ and $A + A^{\bullet-} \rightleftharpoons A^{\bullet-} + A$. Klimkans and Larsson indicated that the reorganization energy of self-exchange ET process is the sum of the energy differences calculated by $\lambda_n = E_{ion}(0) - E_n(0)$ and $\lambda_{ion} = E_n(+1 \text{ or } -1) - E_{ion}(+1 \text{ or } -1)$, where subscripts n and ion indicate geometries optimized for neutral and radical ion forms, respectively, and the number in the parenthesis is the charge [41,42]. Gray and co-workers applied this method to calculate the reorganization energy of zinc porphyrins and compared with the experimentally determined value [43]. They indicated that BHandHLYP reproduces the experimentally determined values. Imahori and co-workers used this method to calculate the reorganization energy of donor–acceptor dyad of porphyrin and perylenediimide (PDI) [44]. They showed that reorganization energy of PDI is larger than that of porphyrin.

We applied this calculation method to the present supramolecular systems. Table 4 summarizes the λ_n, λ_{ion}, and λ_V values for self-exchange ET estimated with B3LYP and BHandHLYP methods using 6-31G(d) basis. The estimated λ_V values are in the order of ZnOEP < ZnHPc < ZnPcn both in the cases of B3LYP and BHandHLYP. This order is maintained also in the pentacoordinated form, which is assuming that a Py ring is coordinated to the central Zn ion in each cases. Larger λ_V values of imides than those of the porphyrinoids are the same tendency as reported by Imahori and co-workers [44]. As shown in the previous papers [23,24,27], in the supramolecular donor–acceptor dyads investigated in this study, HOMO and LUMO electron densities are not distributed on the Py ring in each cases, indicating that the Py ring acts as a spacer. The internal reorganization energy for the ET in the supramolecular dyads should be the sum of λ_V values for self-exchange ET processes of Py coordinated porphyrinoids and acceptors. Thus, the λ_V values for the ET in the supramolecular dyads of ZnOEP, ZnHPc, and ZnPcn are calculated to be 612–719, 682–789, and 887–994 meV, respectively,

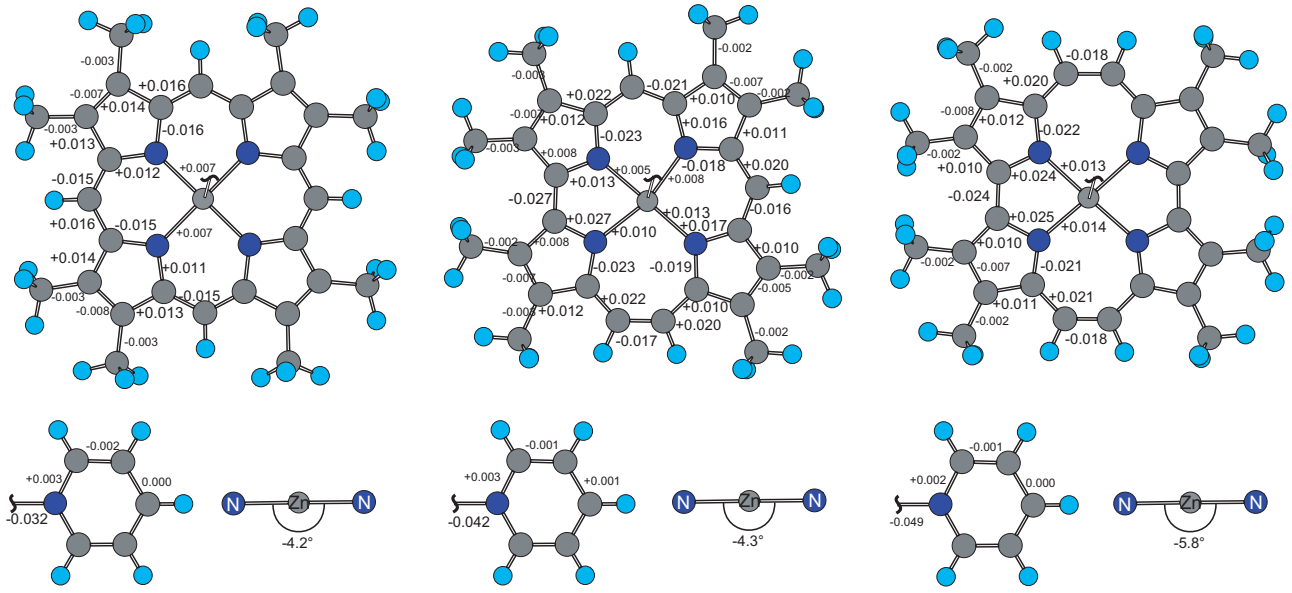

Fig. 5. Difference in the bond length between the neutral and oxidized ZnOEP (left), ZnHPc (center), and ZnPcn (right) coordinated by Py estimated at B3LYP/6-31G(d) level. Large bond length changes were indicated by larger character size. Unit is Å. For simplicity of the calculation, alkyl groups of the compounds were reduced to methyl groups. Difference in N–Zn–N bond angle was also indicated.

using the λ_V values estimated with B3LYP method. These values are 755–844, 777–866, and 1066–1155 meV, respectively, based on BHandHLYP method. In both cases, observed order and differences reproduced experimentally determined λ_V values (Table 3) rather well. The B3LYP gives slightly smaller λ_V values, while the difference in λ_V values is similar to the experimentally determined one. BHandHLYP gives λ_V values close to the experimentally determined for ZnOEP and ZnPcn, while difference between the ZnOEP and ZnHPc seems to be small.

Since the λ_V value is free energy change associated with bond length change during the ET, the difference in the λ_V values of the supramolecular dyads of ZnOEP, ZnHPc, and ZnPcn were investigated from the viewpoint of structural change upon oxidation. In Fig. 5, bond length changes of Py-coordinated ZnOEP, ZnHPc, and ZnPcn upon one electron oxidation were indicated. In each cases, the largest bond length change was observed with the bond between Zn ion and Py ring: the bond became shorter upon oxidation by 0.032–0.049 Å, which is in the same order as the λ_V values. Next large bond length change was observed with the bonds connecting to the α carbon of the pyrrole ring. This is adequate taking the large HOMO electron density on this carbon into account. The changes in the length of the bonds connecting to the α carbon of the pyrrole ring of ZnOEP are smaller than those of ZnPcn and ZnHPc. In addition, the length change of the N–Zn bond is in the order of ZnOEP < ZnHPc < ZnPcn. In each cases, the angle of N–Zn–N became an acute angle upon oxidation. The change in N–Zn–N angle is −4.2°, −4.3°, and −5.8° for ZnOEP, ZnHPc, and ZnPcn, respectively, indicating that Zn ion of ZnPcn is pulled out from the porphyrinoid plain to larger extent than others upon oxidation probably due to smaller inner cavity of ZnPcn than others [45] (N–N distance of

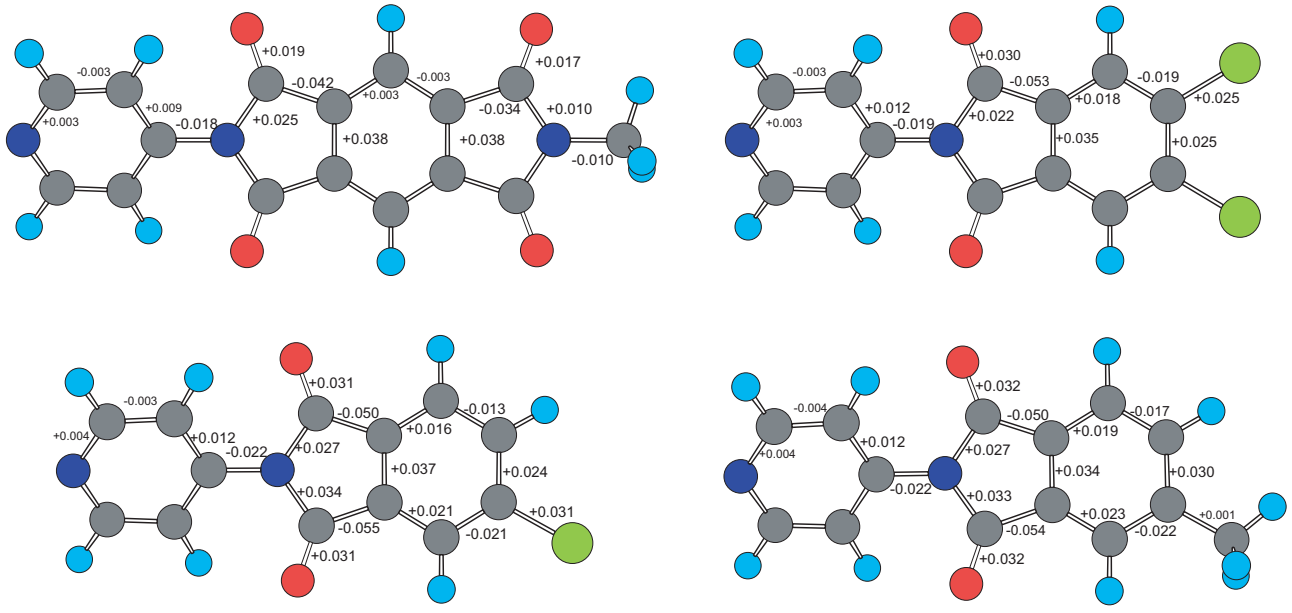

Fig. 6. Difference in the bond length between the neutral and reduced PI (upper left), Cl_2Ph (upper right), ClPh (lower left) and MePh (lower right) estimated at B3LYP/6-31G(d) level. Large bond length changes were indicated by larger character size. Unit is Å. For simplicity of the calculation, alkyl group of PI was reduced to methyl groups.

N–Zn–N is 4.086, 4.047, and 4.011 Å for tetracoordinated neutral ZnOEP, ZnHPc, and ZnPcn, respectively). This point will be rationalized from the calculation on structural change upon oxidation of tetracoordinated ZnOEP, ZnHPc, and ZnPcn, in which ZnPcn showed −2.8° of change in N–Zn–N angle while ZnOEP and ZnHPc did not show angle change keeping planar structure (Supplementary data, Figure S1). Thus, the size of inner cavity will be the one of the factors determining the reorganization energy in the case of Zn coordinated porphyrinoids. Consequently, the difference in changes in the bond length of Py N–Zn ion, bonds around α carbon, and angle around central Zn ion caused difference in the reorganization energies of these porphyrin isomers.

The bond length change upon reduction of the acceptors in this study was indicated in Fig. 6. When compared with the bond length changes of porphyrinoids in Fig. 5, larger bond length changes were observed with these acceptors, in accordance with larger λ_V values of the acceptors as listed in Table 4. In the case of PI, larger bond changes were observed around maleic imide rings, while a benzene ring of phthalimide showed larger changes in the cases of Cl_2Ph, ClPh, and MePh, supporting larger λ_V values of phthalimides. Since the λ_V value of PDI is reported to be 312 meV based on the similar MO calculation [44], delocalization of negative charge over larger π-conjugation systems seems to lower the λ_V value effectively. Furthermore, Cl–C bonds of Cl_2Ph and ClPh showed larger bond length changes upon reduction, which should be the origin of their rather larger λ_V values.

4. Conclusion

In the present paper, we compared the ET processes of supramolecular donor–acceptor dyads of ZnOEP and its isomers, ZnHPc and ZnPcn. First, we investigated ET processes of ZnOEP supramolecular donor–acceptor dyads. The formation of the CS state was successfully observed with the transient absorption spectroscopy. The observed ET rates were compared with those of two porphyrin isomers. The observed difference in the free energy change dependence of ET rates was attributed to the difference in electronic coupling and reorganization energy. The distribution of HOMO electron density gives reasonable explanation on the difference in the electronic coupling. The difference in the reorganization energy was reproduced by MO calculation and a structural factor giving difference in the internal reorganization energy was pointed out. Thus, the application of MO theory to the ET study gives better insight and is useful to design a molecular system applicable to efficient light energy conversion and so on.

Acknowledgments

This work has been partly supported by a Grant-in-Aid for Scientific Research (Project 21350075, 22245022, Priority Area (477), and others) from the Ministry of Education, Culture, Sports, Science and Technology (MEXT) of Japanese Government. T.M. thanks to WCU (World Class University) program through the National Research Foundation of Korea funded by the Ministry of Education, Science and Technology (R31-10035) for the support.

Appendix A. Supplementary data

Supplementary data associated with this article can be found, in the online version, at doi:10.1016/j.jphotochem.2010.10.016.

References

[1] M.R. Wasielewski, Photoinduced electron transfer in supramolecular systems for artificial photosynthesis, Chem. Rev. 92 (1992) 435–461.
[2] R.A. Haycock, C.A. Hunter, D.A. James, U. Michelsen, L.R. Sutton, Self-assembly of oligomeric porphyrin rings, Org. Lett. 2 (2000) 2435–2438.
[3] K. Ogawa, Y. Kobuke, Formation of a giant supramolecular porphyrin array by self-coordination, Angew. Chem. Int. Ed. 39 (2000) 4070–4073.
[4] I.-W. Hwang, H.S. Cho, D.H. Jeong, D. Kim, A. Tsuda, T. Nakamura, A. Osuka, Photophysical properties of a three-dimensional zinc(II) porphyrin box, J. Phys. Chem. B 107 (2003) 9977–9988.
[5] H.L. Anderson, C.A. Hunter, J.K.M. Sanders, Assembly of a photoactive supramolecule using porphyrin coordination chemistry, J. Chem. Soc., Chem. Commun. (1989) 226–227.
[6] C.A. Hunter, J.K. Sanders, G.S. Beddard, S. Evans, A new approach to the assembly of electron donor-spacer-acceptor systems, J. Chem. Soc., Chem. Commun. (1989) 1765–1767.
[7] U. Rempel, B. von Maltzan, C. von Borczyskowski, Temperature and solvent dependent charge transfer in self-organized porphyrin-quinone compounds, Pure Appl. Chem. 65 (1993) 1681–1685.
[8] H. Imahori, E. Yoshizawa, K. Yamada, K. Hagiwara, T. Okada, Y. Sakata, Porphyrin-quinone supramolecule with two coordination bonds, J. Chem. Soc., Chem. Commun. (1995) 1133–1134.
[9] C.A. Hunter, R.K. Hyde, Photoinduced energy and electron transfer in supramolecular porphyrin assemblies, Angew. Chem. Int. Ed. Engl. 35 (1996) 1936–1939.
[10] F. D'Souza, G.R. Deviprasad, M.S. Rahman, J. Choi, Self-Assembled porphyrin-C_{60} and porphycene-C_{60} complexes via metal axial coordination, Inorg. Chem. 38 (1999) 2157–2160.
[11] T. Da Ros, M. Prato, D. Guldi, E. Alessio, M. Ruzzi, L. Pasimeni, A noncovalently linked, dynamic fullerene porphyrin dyad. Efficient formation of long-lived charge separated states through complex dissociation, Chem. Commun. (1999) 635–636.
[12] N. Armaroli, F. Diederich, L. Echegoyen, T. Habicher, L. Falmigni, G. Marconi, J.F. Nierengarten, A new pyridyl-substituted methanofullerene derivative. Photophysics, electrochemistry and self-assembly with zinc(II) meso-tetraphenylporphyrin (ZnTPP), New J. Chem. 23 (1999) 77–83.
[13] D.M. Guldi, C. Luo, T. Da Ross, M. Prato, E. Dietel, A. Hirsh, Photoinduced electron transfer in multicomponent arrays of a π-stacked fullerene porphyrin dyad and diazabicyclooctane or a fulleropyrrolidine ligand, Chem. Commun. (2000) 375–376.
[14] F. D'Souza, N.P. Rath, G.R. Deviprasad, M.E. Zandler, Structural studies of a non-covalently linked porphyrin-fullerene dyad, Chem. Commun. (2001) 267–268.
[15] F. D'Souza, G.R. Deviprasad, M.E. El-Khouly, M. Fujitsuka, O. Ito, Probing the donor–acceptor proximity on the physicochemical properties of porphyrin-fullerene dyads: "Tail-On" and "Tail-Off" binding approach, J. Am. Chem. Soc. 123 (2001) 5277–5284.
[16] L. Flamigni, M.R. Johnston, L. Giribabu, Photoinduced electron transfer in bisporphyrin-diimide complexes, Chem. Eur. J. 8 (2002) 3938–3947.
[17] J. Otsuki, M. Takatsuki, M. Kaneko, H. Miwa, T. Takido, M. Seno, K. Okamoto, H. Imahori, M. Fujitsuka, Y. Araki, O. Ito, S. Fukuzumi, Formation of a supramolecular porphyrin-spacer-acceptor ternary complex and intracomplex electron transfer, J. Phys. Chem. A 107 (2003) 379–385.
[18] M.E. El-Khouly, L.S. Rogers, M.E. Zandler, G. Suresh, M. Fujitsuka, O. Ito, F. D'Souza, Studies on intra-supramolecular and intermolecular electron-transfer processes between zinc naphthalocyanine and imidazole-appended fullerene, ChemPhysChem 4 (2003) 474–481.
[19] F. D'Souza, P.M. Smith, S. Gadde, A.L. McCarty, M.J. Kullman, M.E. Zandler, M. Itou, Y. Araki, O. Ito, Supramolecular triads formed by axial coordination of fullerene to covalently linked zinc porphyrin-ferrocene(s): design, syntheses, electrochemistry, and photochemistry, J. Phys. Chem. B 108 (2004) 11333–11343.
[20] F. D'Souza, P.M. Smith, L. Rogers, M.E. Zandler, D.-M.S. Islam, Y. Araki, O. Ito, Formation, spectral, electrochemical, and photochemical behavior of zinc N-confused porphyrin coordinated to imidazole functionalized fullerene dyads, Inorg. Chem. 45 (2006) 5057–5065.
[21] F. D'Souza, N.K. Subbaiyan, Y. Xie, J.P. Hill, K. Ariga, K. Ohkubo, S. Fukuzumi, Anion-complexation-induced stabilization of charge separation, J. Am. Chem. Soc. 131 (2009) 16138–16146.
[22] J. Otsuki, K. Harada, K. Toyama, Y. Hirose, K. Araki, M. Seno, K. Takatera, T. Watanabe, Energy gap dependence of electron transfer rates in porphyrin-imide supramolecular assemblies, Chem. Commun. (1998) 1515–1516.
[23] M. Fujitsuka, H. Shimakoshi, S. Tojo, L. Cheng, D. Maeda, Y. Hisaeda, T. Majima, Electron transfer in the supramolecular donor–acceptor dyad of zinc porphycene, J. Phys. Chem. A 113 (2009) 3330–3335.
[24] M. Fujitsuka, H. Shimakoshi, S. Tojo, L. Cheng, D. Maeda, Y. Hisaeda, T. Majima, Electron transfer in the supramolecular donor–acceptor dyad of zinc hemiporphycene, J. Phys. Chem. A 114 (2010) 4156–4162.
[25] C.J. Fowler, J.L. Sessler, V.M. Lynch, J. Waluk, A. Gebauer, J. Lex, A. Heger, F. Zuniga-y-Rivero, E. Vogel, Metal complexes of porphycene, corrphycene, and hemiporphycene: stability and coordination chemistry, Chem. Eur. J. 8 (2002) 3485–3496.
[26] C. Bernald, J.P. Gisselbrecht, M. Gross, E. Vogel, M. Lausmann, Redox properties of porphycenes and metalloporphycenes. A comparison with porphyrins, Inorg. Chem. 33 (1994) 2393–2401.
[27] K. Harada, M. Fujitsuka, A. Sugimoto, T. Majima, Electron transfer from the S_1 and S_2 states of pentacoordinated tetrapyrrole macrocycles to pyromellitic diimide as an axial ligand, J. Phys. Chem. A 111 (2007) 11430–11436.

[28] M. Fujitsuka, D.W. Cho, S. Tojo, A. Inoue, T. Shiragami, M. Yasuda, T. Majima, Electron transfer from axial ligand to S_1- and S_2-excited phosphorus tetraphenylporphyrin, J. Phys. Chem. A 111 (2007) 10574–105 79.
[29] M. Fujitsuka, A. Okada, S. Tojo, F. Takei, K. Onitsuka, S. Takahashi, T. Majima, Rapid exciton migration and fluorescent energy transfer in helical polyisocyanides with regularly arranged porphyrin pendants, J. Phys. Chem. B 108 (2004) 11935–11941.
[30] M.J. Frisch, G.W. Trucks, H.B. Schlegel, G.E. Scuseria, M.A. Robb, J.R. Cheeseman, J.A. Montgomery Jr., T. Vreven, K.N. Kudin, J.C. Burant, J.M. Millam, S.S. Iyengar, J. Tomasi, V. Barone, B. Mennucci, M. Cossi, G. Scalmani, N. Rega, G.A. Petersson, H. Nakatsuji, M. Hada, M. Ehara, K. Toyota, R. Fukuda, J. Hasegawa, M. Ishida, T. Nakajima, Y. Honda, O. Kitao, H. Nakai, M. Klene, X. Li, J.E. Knox, H.P. Hratchian, J.B. Cross, V. Bakken, C. Adamo, J. Jaramillo, R. Gomperts, R.E. Stratmann, O. Yazyev, A.J. Austin, R. Cammi, C. Pomelli, J.W. Ochterski, P.Y. Ayala, K. Morokuma, G.A. Voth, P. Salvador, J.J. Dannenberg, V.G. Zakrzewski, S. Dapprich, A.D. Daniels, M.C. Strain, O. Farkas, D.K. Malick, A.D. Rabuck, K. Raghavachari, J.B. Foresman, J.V. Ortiz, Q. Cui, A.G. Baboul, S. Clifford, J. Cioslowski, B.B. Stefanov, G. Liu, A. Liashenko, P. Piskorz, I. Komaromi, R.L. Martin, D.J. Fox, T. Keith, M.A. Al-Laham, C.Y. Peng, A. Nanayakkara, M. Challacombe, P.M.W. Gill, B. Johnson, W. Chen, M.W. Wong, C. Gonzalez, J.A. Pople, Gaussian 03, Revision E.01, Gaussian, Inc., Wallingford, CT, 2004.
[31] G. Scatchard, The attraction of proteins for small molecules and ions, Ann. NY Acad. Sci. 51 (1949) 660–672.
[32] A. Weller, Photoinduced electron transfer in solution: exciplex and radical ion pair formation free enthalpies and their solvent dependence, Zeit. Phys. Chem. Neue Folge 133 (1982) 93–98.
[33] N. Mataga, H. Chosrowjan, S. Taniguchi, Y. Shibata, N. Yoshida, A. Osuka, T. Kikuzawa, T. Okada, Ultrafast charge separation from the S_2 excited state of directly linked porphyrin-imide dyads: first unequivocal observation of the whole bell-shaped energy-gap law and its solvent dependencies, J. Phys. Chem. A 106 (2002) 12191–12201.
[34] J.H. Fuhrhop, P. Wasser, D. Riesner, D. Mauzerall, Dimerization and π-bonding of a zinc porphyrin cation radical. Thermodynamics and fast reaction kinetics, J. Am. Chem. Soc. 94 (1972) 7996–8001.
[35] R.A. Marcus, Chemical and electrochemical electron-transfer theory, Annu. Rev. Phys. Chem. 15 (1964) 155–196.
[36] R.A. Marcus, N. Sutin, Electron transfers in chemistry and biology, Biochim. Biophys. Acta 811 (1985) 265–322.
[37] D. Holten, D.F. Bocian, J.S. Lindsey, Probing electronic communication in covalently linked multiporphyrin arrays. A guide to the rational design of molecular photonic devices, Acc. Chem. Res. 35 (2002) 57–69.
[38] R.T. Hayes, C.J. Walsh, M.R. Wasielewski, Competitive electron transfer from the S_2 and S_1 excited states of zinc meso-tetraphenylporphyrin to a covalently bound pyromellitimide: dependence on donor–acceptor structure and solvent, J. Phys. Chem. A 108 (2004) 2375–2381.
[39] C. Weiss, H. Kobayashi, M. Gouterman, Spectra of porphyrins. III. Self-consistent molecular orbital calculations of porphyrin and related ring systems, J. Mol. Spectrosc. 16 (1965) 415–450.
[40] G.J. Kavarnos, N.J. Turro, Photosensitization by reversible electron transfer: theories, experimental evidence, and examples, Chem. Rev. 86 (1986) 401–449.
[41] A. Klimkans, S. Larsson, Reorganization energies in benzene, naphthalene, and anthracene, Chem. Phys. 189 (1994) 25–31.
[42] A. Amini, A. Harriman, Computational methods for electron-transfer systems, J. Photochem. Photobiol. C: Photochem. Rev. 4 (2003) 155–177.
[43] X. Amashukeli, N.E. Gruhn, D.L. Lichtenberger, J.R. Winkler, H.B. Gray, Inner-sphere electron-transfer reorganization energies of zinc porphyrins, J. Am. Chem. Soc. 126 (2004) 15566–15571.
[44] Y. Shibano, T. Umeyama, Y. Matano, N.V. Tkachenko, H. Lemmetyinen, Y. Araki, O. Ito, H. Imahori, Large reorganization energy of pyrrolidine-substituted perylenediimide in electron transfer, J. Phys. Chem. C 111 (2007) 6133–6142.
[45] J. Waluk, Ground- and excited-state tautomerism in porphycenes, Acc. Chem. Res. 39 (2006) 945–952.